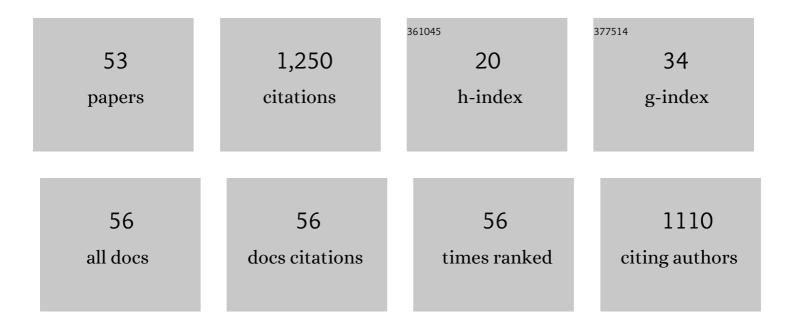
Nathan A S Webster

List of Publications by Year in descending order

Source: https://exaly.com/author-pdf/7931623/publications.pdf Version: 2024-02-01



#	Article	IF	CITATIONS
1	Fundamentals of Silico-Ferrite of Calcium and Aluminium (SFCA) and SFCA-I Iron Ore Sinter Bonding Phase Formation: Effects of MgO Source on Phase Formation during Heating. ISIJ International, 2022, 62, 652-657.	0.6	0
2	Fundamentals of Silico-Ferrite of Calcium and Aluminum (SFCA) and SFCA-I Iron Ore Sinter Bonding Phase Formation: Effects of MgO on Phase Formation During Heating. Jom, 2021, 73, 299-305.	0.9	11
3	Effect of Temperature, Time, and Cooling Rate on the Mineralogy, Morphology, and Reducibility of Iron Ore Sinter Analogues. Jom, 2021, 73, 345-355.	0.9	13
4	Anatomy of a complex mineral replacement reaction: Role of aqueous redox, mineral nucleation, and ion transport properties revealed by an in-situ study of the replacement of chalcopyrite by copper sulfides. Chemical Geology, 2021, 581, 120390.	1.4	10
5	Kinetics and Mechanisms of Carbothermic Reduction of Weathered Ilmenite Using Palm Kernel Shell Biomass. Journal of Sustainable Metallurgy, 2021, 7, 1819-1837.	1.1	5
6	Raman Spectroscopy of Formamidinium-Based Lead Halide Perovskite Single Crystals. Journal of Physical Chemistry C, 2020, 124, 2265-2272.	1.5	44
7	Investigation of the Internal Structure of a Modern Seafloor Hydrothermal Chimney With a Combination of EBSD, EPMA, and XRD. Microscopy and Microanalysis, 2020, 26, 793-807.	0.2	3
8	Steady-state electrochemical synthesis of HKUST-1 with polarity reversal. Microporous and Mesoporous Materials, 2020, 303, 110218.	2.2	19
9	Fundamentals of Silico-Ferrite of Calcium and Aluminium (SFCA) Iron Ore Sinter Bonding Phase Formation: Effects of Titanium on Crystallisation during Cooling. ISIJ International, 2019, 59, 1007-1010.	0.6	14
10	Characterisation of phosphorus and other impurities in goethite-rich iron ores – Possible P incorporation mechanisms. Minerals Engineering, 2019, 143, 106022.	1.8	18
11	Fundamentals of Silico-Ferrite of Calcium and Aluminium (SFCA) Iron Ore Sinter Bonding Phase Formation: Effects of Basicity and Magnesium on Crystallisation during Cooling. ISIJ International, 2019, 59, 263-267.	0.6	26
12	Evidence of anatase intergrowths formed during slow cooling of reduced ilmenite. Journal of Applied Crystallography, 2018, 51, 185-192.	1.9	3
13	High temperature oxidation of rare earth permanent magnets. Part 1 – Microstructure evolution and general mechanism. Corrosion Science, 2018, 133, 374-385.	3.0	31
14	A Review of the Chemistry, Structure and Formation Conditions of Silico-Ferrite of Calcium and Aluminum (â€~SFCA') Phases. ISIJ International, 2018, 58, 2157-2172.	0.6	65
15	Thermodynamic stability of <scp>SFCA</scp> (silicoâ€ferrite of calcium and aluminum) and <scp>SFCA</scp> â€f phases. Journal of the American Ceramic Society, 2017, 100, 3646-3651.	1.9	10
16	The effect of thermal pre-treatment on the dissolution of chalcopyrite (CuFeS2) in sulfuric acid media. Hydrometallurgy, 2017, 169, 68-78.	1.8	20
17	A flow cell for the study of gas-solid reactions via <i>in situ</i> powder X-ray diffraction. Review of Scientific Instruments, 2017, 88, 105104.	0.6	2
18	Fundamentals of silico-ferrite of calcium and aluminium (SFCA) and SFCA-I iron ore sinter bonding phase formation: effects of mill scale addition. Powder Diffraction, 2017, 32, S85-S89.	0.4	6

NATHAN A S WEBSTER

#	Article	IF	CITATIONS
19	<i>In situ</i> XRD investigation of the evolution of surface layers on Pb-alloy anodes. Powder Diffraction, 2017, 32, S54-S60.	0.4	1
20	Predicting iron ore sinter strength through partial least square regression (PLSR) analysis of X-ray diffraction patterns. Powder Diffraction, 2017, 32, S66-S69.	0.4	2
21	Effects of Gibbsite, Kaolinite and Al-rich Goethite as Alumina Sources on Silico-Ferrite of Calcium and Aluminium (SFCA) and SFCA-I Iron Ore Sinter Bonding Phase Formation. ISIJ International, 2017, 57, 41-47.	0.6	40
22	Effects of Sintering Materials and Gas Conditions on Formation of Silico-Ferrites of Calcium and Aluminium during Iron Ore Sintering. ISIJ International, 2016, 56, 1138-1147.	0.6	27
23	Fundamentals of Silico-Ferrite of Calcium and Aluminium (SFCA) and SFCA-I Iron Ore Sinter Bonding Phase Formation: Effects of Titanomagnetite-based Ironsand and Titanium Addition. ISIJ International, 2016, 56, 1715-1722.	0.6	29
24	Effect of Addition of Mill Scale on Sintering of Iron Ores. Metallurgical and Materials Transactions B: Process Metallurgy and Materials Processing Science, 2016, 47, 2848-2860.	1.0	4
25	Vacancy Generation and Oxygen Uptake in Cu-Doped Pr-CeO ₂ Materials using Neutron and in Situ X-ray Diffraction. Inorganic Chemistry, 2016, 55, 12595-12602.	1.9	13
26	Behavior of New Zealand Ironsand During Iron Ore Sintering. Metallurgical and Materials Transactions B: Process Metallurgy and Materials Processing Science, 2016, 47, 330-343.	1.0	32
27	Controllable synthesis of VO ₂ (D) and their conversion to VO ₂ (M) nanostructures with thermochromic phase transition properties. Inorganic Chemistry Frontiers, 2016, 3, 1035-1042.	3.0	55
28	The influence of ore composition on sinter phase mineralogy and strength. Institutions of Mining and Metallurgy Transactions Section C: Mineral Processing and Extractive Metallurgy, 2016, 125, 140-148.	0.6	24
29	Phase and morphology evolution during the solvothermal synthesis of VO2 polymorphs. Inorganic Chemistry Frontiers, 2016, 3, 117-124.	3.0	20
30	In situsynchrotron X-ray diffraction investigation ofÂthe evolution of a PbO2/PbSO4surface layer onÂaÂcopper electrowinning Pb anode in a novel electrochemical flow cell. Journal of Synchrotron Radiation, 2015, 22, 366-375.	1.0	12
31	Synthesis and formation mechanism of VO ₂ (A) nanoplates with intrinsic peroxidase-like activity. RSC Advances, 2015, 5, 61371-61379.	1.7	42
32	Characterisation of the phase-transformation behaviour of Ce ₂ 0(CO ₃) ₂ ·H ₂ 0 clusters synthesised from Ce(NO ₃) ₃ ·6H ₂ 0 and urea. Powder Diffraction, 2014, 29, S84-S88.	0.4	4
33	In situ diffraction studies of iron ore sinter bonding phase formation: QPA considerations and pushing the limits of laboratory data collection. Powder Diffraction, 2014, 29, S54-S58.	0.4	8
34	Structure–property relationships in fluorite-type Bi ₂ O ₃ –Yb ₂ O ₃ –PbO solid-electrolyte materials. Powder Diffraction, 2014, 29, S73-S77.	0.4	0
35	In situ X-ray diffraction analysis of the onset of mineral scale deposition from synthetic oilfield processing waters. Fuel, 2014, 137, 211-215.	3.4	7
36	Fundamentals of Silico-Ferrite of Calcium and Aluminum (SFCA) and SFCA-I Iron Ore Sinter Bonding Phase Formation: Effects of CaO:SiO2 Ratio. Metallurgical and Materials Transactions B: Process Metallurgy and Materials Processing Science, 2014, 45, 2097-2105.	1.0	76

NATHAN A S WEBSTER

#	Article	IF	CITATIONS
37	Kinetics of the Thermally-Induced Structural Rearrangement of γ-MnO ₂ . Journal of Physical Chemistry C, 2014, 118, 24257-24265.	1.5	14
38	Cu2ZnGeS4 Nanocrystals from Air-Stable Precursors for Sintered Thin Film Alloys. Chemistry of Materials, 2014, 26, 5482-5491.	3.2	42
39	Non-injection synthesis of Cu ₂ ZnSnS ₄ nanocrystals using a binary precursor and ligand approach. RSC Advances, 2013, 3, 1017-1020.	1.7	38
40	In Situ Formation of Reactive Sulfide Precursors in the One-Pot, Multigram Synthesis of Cu ₂ ZnSnS ₄ Nanocrystals. Crystal Growth and Design, 2013, 13, 1712-1720.	1.4	57
41	In situ X-ray Diffraction Investigation of the Formation Mechanisms of Silico-Ferrite of Calcium and Aluminium-I-type (SFCA-I-type) Complex Calcium Ferrites. ISIJ International, 2013, 53, 1334-1340.	0.6	56
42	Effect of Oxygen Partial Pressure on the Formation Mechanisms of Complex Ca-rich Ferrites. ISIJ International, 2013, 53, 774-781.	0.6	74
43	Weathered Ilmenite: Diverse Mechanisms of Sintering and Association with Contaminants. Australian Journal of Chemistry, 2012, 65, 892.	0.5	0
44	An in situ synchrotron X-ray diffraction investigation of lepidocrocite and ferrihydrite-seeded Al(OH)3 crystallisation from supersaturated sodium aluminate liquor. Journal of Crystal Growth, 2012, 340, 112-117.	0.7	8
45	Silico-ferrite of Calcium and Aluminum (SFCA) Iron Ore Sinter Bonding Phases: New Insights into Their Formation During Heating and Cooling. Metallurgical and Materials Transactions B: Process Metallurgy and Materials Processing Science, 2012, 43, 1344-1357.	1.0	148
46	Quantitative Phase Analysis. NATO Science for Peace and Security Series B: Physics and Biophysics, 2012, , 207-218.	0.2	8
47	New quenched-in fluorite-type materials in the Bi2O3–La2O3–PbO system: Synthesis and complex phase behaviour up to 750°C. Materials Research Bulletin, 2011, 46, 538-542.	2.7	2
48	An investigation of the mechanisms of goethite, hematite and magnetite-seeded Al(OH)3 precipitation from synthetic Bayer liquor. Hydrometallurgy, 2011, 109, 72-79.	1.8	18
49	An investigation of goethite-seeded Al(OH) ₃ precipitation using <i>in situ</i> X-ray diffraction and Rietveld-based quantitative phase analysis. Journal of Applied Crystallography, 2010, 43, 466-472.	1.9	15
50	A flow cell forin situsynchrotron x-ray diffraction studies of scale formation under Bayer processing conditions. Review of Scientific Instruments, 2009, 80, 084102.	0.6	11
51	X-Ray reflectometry studies on the effect of water on the surface structure of [C4mpyr][NTf2] ionic liquid. Physical Chemistry Chemical Physics, 2009, 11, 11507.	1.3	41
52	The structural and conductivity evolution of fluorite-type Bi2O3–Er2O3–PbO solid electrolytes during long-term annealing. Solid State Ionics, 2008, 179, 697-705.	1.3	11
53	The structure and conductivity of new fluorite-type Bi2O3–Er2O3–PbO materials. Solid State Ionics, 2007, 178, 1451-1451.	1.3	11